Divalent Cations Regulate Connexin Hemichannels by Modulating Intrinsic Voltage-dependent Gating

Vytas K. Verselis[1] and Miduturu Srinivas[2]

[1]Albert Einstein College of Medicine, Bronx, NY 10561
[2]SUNY State College of Optometry, New York, NY 10036

Connexin hemichannels are robustly regulated by voltage and divalent cations. The basis of voltage-dependent gating, however, has been questioned with reports that it is not intrinsic to hemichannels, but rather is derived from divalent cations acting as gating particles that block the pore in a voltage-dependent manner. Previously, we showed that connexin hemichannels possess two types of voltage-dependent gating, termed V_j and loop gating, that in Cx46 operate at opposite voltage polarities, positive and negative, respectively. Using recordings of single Cx46 hemichannels, we found both forms of gating persist in solutions containing no added Mg^{2+} and EGTA to chelate Ca^{2+}. Although loop gating persists, it is significantly modulated by changing levels of extracellular divalent cations. When extracellular divalent cation concentrations are low, large hyperpolarizing voltages, exceeding -100 mV, could still drive Cx46 hemichannels toward closure. However, gating is characterized by continuous flickering of the unitary current interrupted by occasional, brief sojourns to a quiet closed state. Addition of extracellular divalent cations, in this case Mg^{2+}, results in long-lived residence in a quiet closed state, suggesting that hyperpolarization drives the hemichannel to close, perhaps by initiating movements in the extracellular loops, and that divalent cations stabilize the fully closed conformation. Using excised patches, we found that divalent cations are only effective from the extracellular side, indicative that the binding site is not cytoplasmic or in the pore, but rather extracellular. V_j gating remains essentially unaffected by changing levels of extracellular divalent cations. Thus, we demonstrate that both forms of voltage dependence are intrinsic gating mechanisms in Cx46 hemichannels and that the action of external divalent cations is to selectively modulate loop gating.

INTRODUCTION

It is now evident that connexin hemichannels (connexons) are functional when unapposed or undocked, operating in the plasma membrane like conventional ion channels. Analogous to their cell–cell or gap junction channel counterparts, hemichannels constitute large ion channels that are capable of mediating fluxes of a variety of signaling molecules. Reported functions of hemichannels include mediating the release of glutamate and ATP (Stout et al., 2002; Ye et al., 2003; Zhao et al., 2005; Genetos et al., 2007; Schock et al., 2008), the spread of Ca^{2+} waves (Weissman et al., 2004), and negative feedback from horizontal cells to cones in the vertebrate retina (Kamermans et al., 2001; Kamermans and Fahrenfort, 2004). Recently, hemichannels formed of the functionally related pannexin genes were reported to act as ATP release channels when coupled to purinergic P2Y receptors (Locovei et al., 2006; Pelegrin and Surprenant, 2006; Huang et al., 2007) and to contribute to neuronal excitotoxicity after ischemia, suggesting a role in mediating loss of cell metabolites and/or entry of extracellular ions during stroke (Thompson et al., 2006).

Due to the large size of the aqueous pore, hemichannel opening in the plasma membrane ought to be highly

regulated. A relatively small number of open hemichannels can have a large impact on a cell's electrical properties, and unregulated opening of hemichannels can be deleterious to a cell's integrity due to excessive loss of intracellular constituents and influx of extracellular ions. Initial studies of hemichannels expressed in *Xenopus* oocytes were those of Cx46 and showed large, time and voltage-dependent currents that activated with depolarization; extracellular divalent cations strongly inhibited the currents and shifted activation to more positive potentials (Ebihara and Steiner, 1993). Subsequent studies of hemichannels formed of a variety of connexins have shown qualitatively similar properties, i.e., voltage and extracellular divalent cations are potent regulators with hyperpolarization and elevated levels of divalent cations generally promoting closure. However, it was reported that voltage-dependent gating in Cx46 hemichannels is lost in solutions containing no added divalent cations, suggesting that divalent cations are required for gating (Ebihara et al., 2003). Similarly, loss of gating was reported in Cx37 hemichannels upon removal of divalent cations from the bath solution and a

model was proposed whereby extracellular divalent cations produce voltage-dependent block by traversing the pore and binding to a site located at the cytoplasmic end of the hemichannel (Puljung et al., 2004). In both cases, it was concluded that there is no intrinsic voltage gate and that voltage dependence can be explained solely by divalent cation block/unblock.

Thus far, studies reporting loss of voltage gating in hemichannels have relied solely on macroscopic recordings of connexins expressed in *Xenopus* oocytes where there is the possibility of series access resistance errors (Baumgartner et al., 1999) resulting from the large membrane conductances that typically accompany removal of divalent cations. These studies also did not consider the complexity of connexin hemichannel gating, specifically that there are two principal types of gating, one that closes hemichannels to a long-lived substate, termed V_j or fast gating, and one that closes them fully, termed loop or slow gating (Bukauskas and Verselis, 2004). V_j gating is the mechanism originally described in gap junction channels in response to transjunctional voltages, V_j. Loop gating was named provisionally because of the plausible involvement of the extracellular loops in closing hemichannels (Trexler et al., 1996). Both forms of gating appear to be properties that are common to all connexin channels and hemichannels (Bukauskas and Verselis, 2004).

Here we sought to examine the relationship between divalent cations and both V_j and loop gating by making use of single hemichannel recordings. We focused on Cx46 hemichannels in which V_j and loop gating have been shown to operate at opposite voltage polarities, positive and negative, respectively (Trexler et al., 1996). Also, single hemichannel recordings permitted unambiguous distinction between V_j and loop gating events, circumvented series access resistance problems, and allowed examination of hemichannels in isolation without contaminating endogenous *Xenopus* channels. We demonstrate that both forms of voltage gating are intrinsic voltage-dependent mechanisms in Cx46 hemichannels and that the action of external divalent cations is inconsistent with open channel block. Rather, divalent cations act as modifiers of intrinsic gating, selectively acting on loop gating by promoting stable, long-lived closures with membrane hyperpolarization.

MATERIALS AND METHODS

Expression of Cx46 in *Xenopus* Oocytes
Cx46 DNA was cloned from rat genomic DNA using PCR amplification with primers corresponding to amino- and carboxy-terminal sequences as described previously (Trexler et al., 1996). Synthesis of RNA and preparation and injection of oocytes have been described previously (Trexler et al., 1996, 2000). Injected oocytes were kept at 18°C in a modified ND96 solution containing (in mM) 88 NaCl, 1 KCl, 1 MgCl$_2$, 1.8 CaCl$_2$, 5 glucose, 5 HEPES, 5 pyruvate pH 7.6.

Electrophysiological Recordings
To record macroscopic hemichannel currents, *Xenopus* oocytes were placed in a polycarbonate RC-1Z recording chamber (Warner Instruments) with a slot-shaped bath connecting inflow and outflow compartments to allow for rapid perfusion. A suction tube was placed in the outflow compartment and a separate reservoir was used for grounding, connected to the main chamber with an agar bridge. At the start of each experiment, oocytes were bathed in the modified ND96 solution (MND96). Perfusion solutions consisted of MND96 to which Ca^{2+} and or Mg^{2+} concentrations were adjusted to desired levels. 0 Ca^{2+} and 0 Mg^{2+} solutions refer to nominal conditions in which no CaCl$_2$ or MgCl$_2$ was added. I-V curves at each concentration of Ca^{2+} and Mg^{2+} were obtained by applying slow voltage ramps (3 min) from +50 to −100 mV from a holding potential of −40 mV. The data were acquired at 1 kHz. Conductance was calculated as $I/(V_m − V_{rev})$, where V_{rev} is the reversal potential. For the G-V plots, the digitized data were decimated and plotted as points; data points around V_{rev}, which represents a discontinuity, were discarded, giving the curves a continuous appearance. All recordings were obtained with a GeneClamp 500 two-electrode voltage clamp (Axon Instruments). Both current-passing and voltage-recording pipettes contained 1 M KCl. To record single hemichannel currents, *Xenopus* oocytes were manually devitellinized in a hypertonic solution consisting of (in mM) 220 Na aspartate, 10 KCl, 2 MgCl$_2$, 10 HEPES and then placed in MND96 solution for recovery. Oocytes were then individually moved to the recording chamber containing the patch pipette solution (IPS), which consisted of (in mM) 140 KCl, 1 MgCl$_2$, 5 HEPES, 1 CaCl$_2$, 3 EGTA, and pH adjusted to 7.6 with KOH. The recording compartment was connected via a 3 M agar bridge to a ground compartment. To examine the effects of divalent cations, the Mg^{2+} concentration was altered. For experiments using excised patches, changes in the bath solution for any given patch were accomplished through an inflow tube. Bath volume was ∼0.3–0.4 ml and total volume exchange occurred within 5–10 s. Using MaxChelator (http://maxchelator.stanford.edu), free Ca^{2+} and Mg^{2+} levels in our IPS solution were calculated to be ∼2 nM and 1 mM, respectively. IPS solutions in which Mg^{2+} was omitted or raised to 10 mM did not appreciably change free Ca^{2+}.

Single channel records from voltage steps and ramps were leak subtracted by measuring leak conductance of a given patch from full closing transitions and extrapolating linearly with voltage. Single hemichannel I-V curves were obtained by applying 8-s voltage ramps from −70 to +70 mV. To measure open probability in patches containing single hemichannels, currents from patches held at a constant voltage were idealized using the Sublevel Hinkley Detector, SHD (Draber and Schultze, 1994; Trexler et al., 1999). The SHD was set to consider only two levels, fully open and closed, which results in the SHD acting as a half-height threshold algorithm. The SHD was set at low sensitivity to avoid detection of brief, incomplete, noisy events from the closed state. Thus, the closed dwell times incorporated not only the time spent fully closed, but also the time spent flickering around the closed state. Dwell times in the two states were compiled and Po was calculated by summing the dwell times in the open state and dividing by the total recording time. All currents in cell-attached and excised-patch configurations were recorded using an Axopatch 1D amplifier (Axon Instruments Inc.). Currents were filtered at 1 kHz and data were acquired at 5 kHz. All recordings, both macroscopic and at the single hemichannel level were acquired using an AT-MIO-16X D/A board from National Instruments and our own acquisition software (written by E. Brady Trexler). All chemicals were purchased from Sigma-Aldrich.
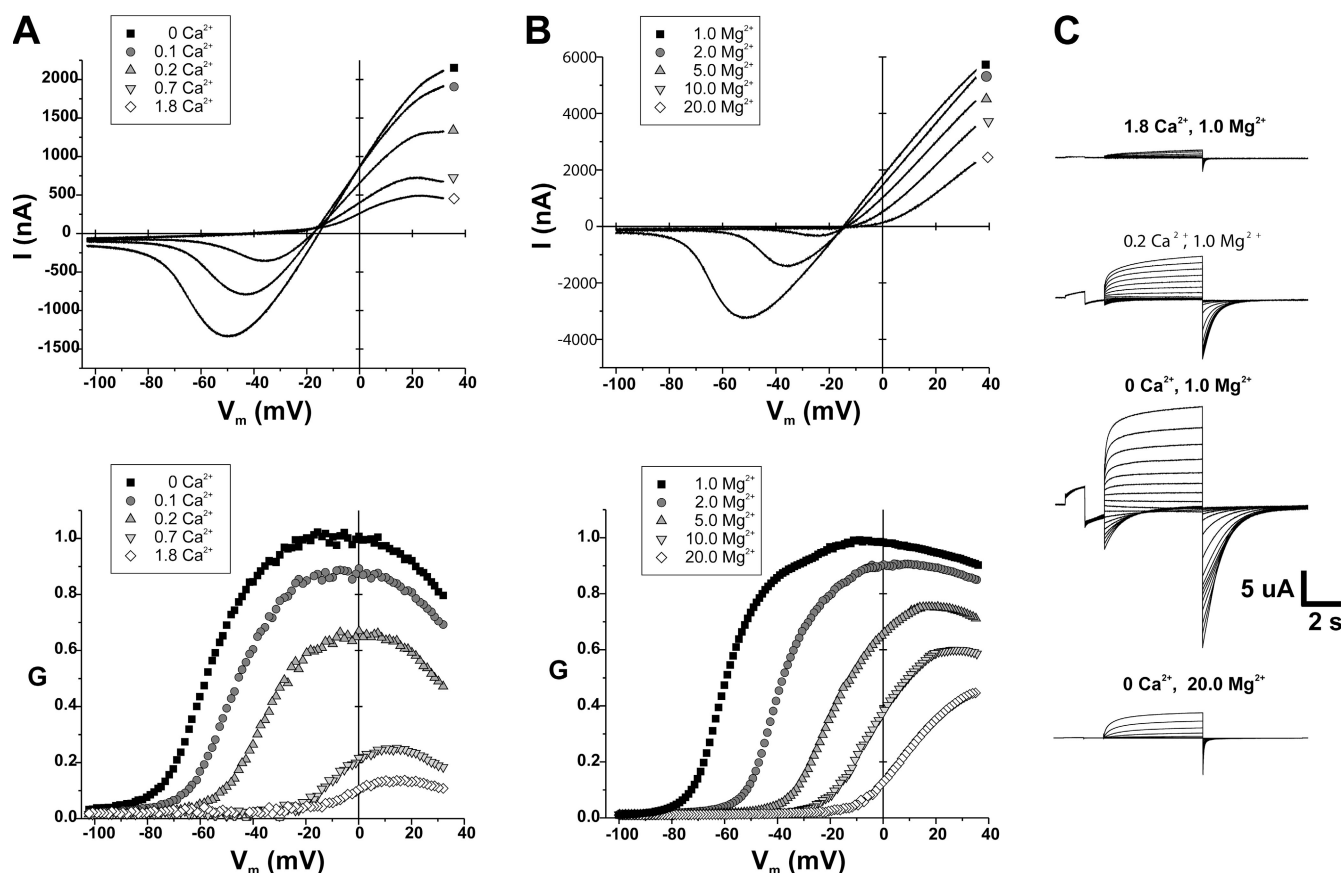
Figure 1. Regulation of macroscopic Cx46 currents by external Ca^{2+} and Mg^{2+}. (A) Representative current–voltage (I-V) relationships (top) at different external Ca^{2+} concentrations ranging from nominal (0 added) to 1.8 mM were obtained by applying slow (3 min) voltage ramps from +50 to −100 mV to a Cx46-expressing oocyte. The holding potential before and after the ramp was −40 mV. For each curve, external Mg^{2+} was maintained at 1 mM. The corresponding conductance–voltage (G-V) relationships are plotted below and show that conductance is maximum at or near 0 mV and decreases asymmetrically with voltages of either polarity. Conductance decreases robustly with hyperpolarization, but only modestly with depolarization. Increasing the extracellular Ca^{2+} concentration caused a significant decrease in overall conductance and led to a substantial rightward shift in voltage sensitivity at negative, but not positive potentials. (B) I-V (top) and corresponding G-V (bottom) relationships obtained at different external Mg^{2+} concentrations ranging from 1 to 20 mM. External Ca^{2+} was maintained at nominal levels. Increasing external Mg^{2+}, like Ca^{2+}, decreased overall conductance and caused a significant positive shift in voltage sensitivity at negative potentials. However, these changes required considerably higher concentrations of Mg^{2+}. (C) Shown are representative currents obtained at different concentrations of external Ca^{2+} and Mg^{2+}. Oocytes were clamped to a holding potential of −40 mV and 5-s voltage steps were applied from +60 to −100 mV followed by a 5-s step to −120. The currents were normalized to a constant prepulse (+10 mV) that preceded each episode. Both Ca^{2+} and Mg^{2+} had similar effects, suppressing the magnitude of the current, slowing activation and speeding up deactivation.

RESULTS

Regulation of Macroscopic Cx46 Currents by External Ca^{2+} and Mg^{2+}

Fig. 1 shows representative Cx46 hemichannel current–voltage relations obtained by applying slow voltage ramps to oocytes in a two-electrode voltage clamp recording configuration. The curves in Fig. 1 A were obtained in external Ca^{2+} concentrations ranging from 1.8 to 0 mM (nominal). External Mg^{2+} was held constant at 1 mM. The corresponding conductance–voltage relations at each Ca^{2+} concentration are plotted below. Overall, the magnitude of the conductance progressively increased as the external Ca^{2+} concentration decreased. At each Ca^{2+} concentration, conductance declined robustly with

hyperpolarization, but sensitivity to voltage shifted substantially such that the voltage at which conductance reached half-maximal shifted from approximately −10 mV in 1.8 mM Ca^{2+} to approximately −60 mV in 0 mM (nominal) Ca^{2+}. Conductance also declined at positive voltages, but more modestly than at negative voltages and with no appreciable shift in voltage sensitivity with changes in external Ca^{2+}. Lowering external Mg^{2+} while maintaining external Ca^{2+} constant at 1.8 mM had little effect on Cx46 hemichannel currents (unpublished data). However, upon lowering external Ca^{2+} to nominal levels (0 added), the effects of external Mg^{2+} were clearly evident and were qualitatively similar to those of external Ca^{2+}, i.e., causing changes in the magnitude of the conductance and large shifts in the G-V relations at
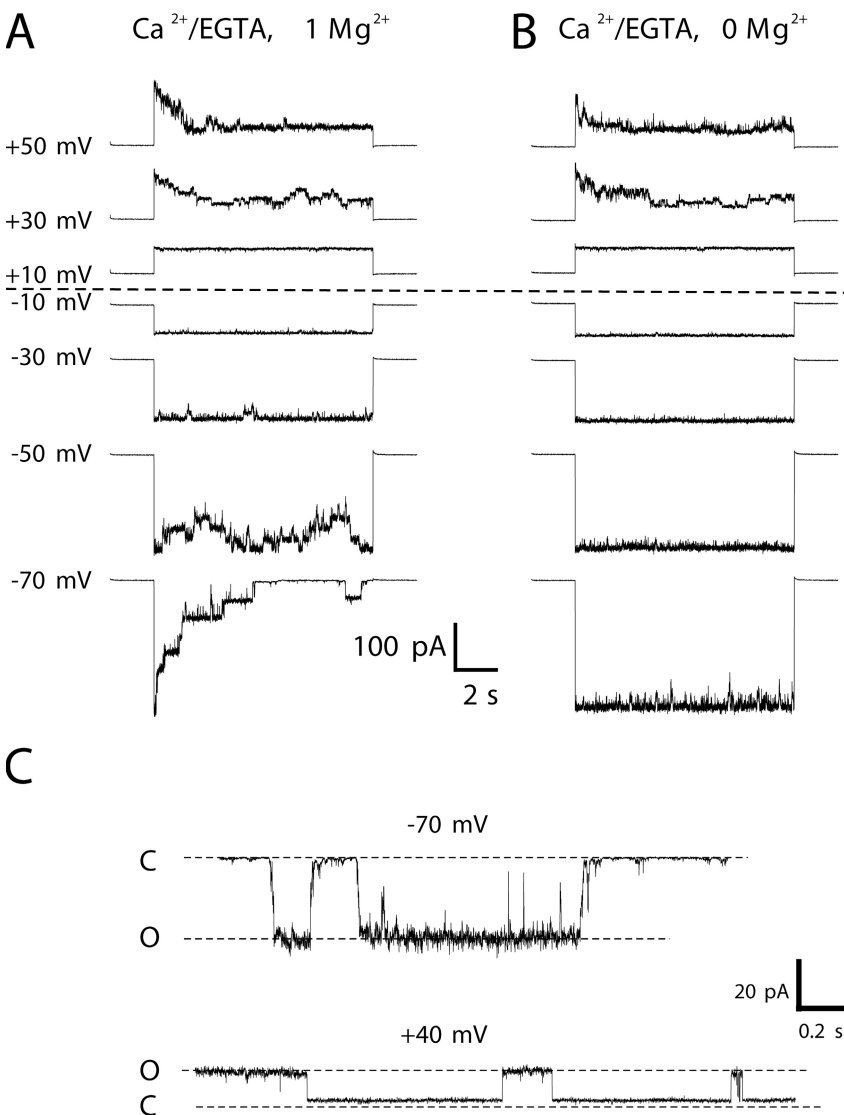
A

Ca²⁺/EGTA, 1 Mg²⁺

B

Ca²⁺/EGTA, 0 Mg²⁺

C

Figure 2. Divalent cations selectively affect gating of Cx46 hemichannels at negative membrane potentials. (A and B) Multichannel cell-attached patch recordings from a Cx46-expressing oocyte recorded with (A) 1 mM Mg²⁺ present in the patch pipette and (B) no added Mg²⁺ in the patch pipette. In both cases, Ca²⁺ was buffered to very low levels with EGTA (Materials and methods). Shown are currents in response to 10-s voltage steps from −70 and +50 mV applied in 20-mV increments. No endogenous channel activity was present these patches. In the presence of 1 mM external Mg²⁺, Cx46 hemichannels essentially remained open at modest voltages (see traces at −10 and +10 mV) and tended to close for either polarity of membrane voltages. Hyperpolarization led to full and robust closure (see trace at −70 mV), whereas depolarization left a residual current (see current trace at +50 mV). The current records were leak subtracted as described in the Materials and methods. When there was no added external Mg²⁺, gating at positive voltages did not change, whereas gating at negative voltages changed significantly. In the example shown, gating was essentially abolished at hyperpolarizing voltages up to −70 mV. (C) Cell-attached patch recordings of single Cx46 hemichannels highlighting the two different types of gating at negative (−70 mV) and positive (+40 mV) voltages, termed loop gating and V_j gating, respectively. Recordings were obtained with standard IPS (containing 1 mM Mg²⁺). Loop gating is characterized by gating transitions between fully closed (C) and open (O) states (left), whereas V_j gating transitions occur between the open state (O) and a long-lasting subconductance state (right). Currents were leak subtracted as described in Materials and methods. All currents were filtered at 1 kHz and data were acquired at 5 kHz.

negative voltages and little or no effect at positive voltages (Fig. 1 B). Representative currents obtained from a family of voltage steps are shown in Fig. 1 C. Raising extracellular Ca²⁺ or Mg²⁺ substantially reduced the magnitude of the Cx46 currents, slowed activation, and sped up deactivation, consistent with previous reports (Ebihara and Steiner, 1993; Ebihara et al., 2003). Thus, both divalent cations appear to regulate Cx46 hemichannels similarly with Ca²⁺ being considerably more potent as previously reported (Ebihara and Steiner, 1993; Ebihara et al., 2003).

Patch Clamp Recording of Cx46 Hemichannels Shows Robust Gating in Low Divalent Cation Conditions

Placing Cx46-expressing oocytes in a solution containing no added Ca²⁺ and Mg²⁺ produced very large membrane currents that displayed little voltage dependence, even with hyperpolarizing voltages exceeding −100 mV

(unpublished data). Concerned that series access resistance could lead to an apparent weakening or loss of voltage dependence and that activation of other endogenous currents could contribute to the appearance of altered voltage dependence, we recorded from cell-attached and excised patches where series access problems were circumvented and where the hemichannels could be observed in isolation; patches containing other endogenous channel activity were discarded. In some cases expression was high enough that patches solely contained multiple Cx46 hemichannels as shown in Fig. 2. Under conditions in which external Mg²⁺ was maintained at 1 mM and external Ca²⁺ was brought to submicromolar levels by addition of EGTA, Cx46 hemichannels closed robustly with hyperpolarization. In the example shown in Fig. 2 A, Cx46 hemichannels were essentially open at small negative membrane potentials and hyperpolarization beyond −40 mV initiated closure; at a voltage of
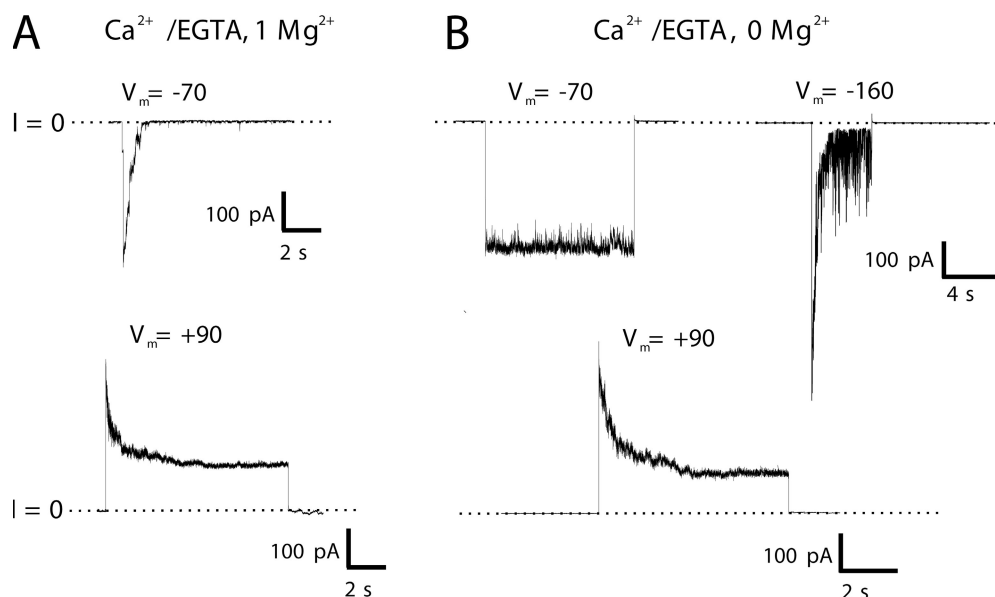
A Ca²⁺/EGTA, 1 Mg²⁺

$V_m = -70$

I = 0

100 pA

2 s

$V_m = +90$

I = 0

100 pA

2 s

B Ca²⁺/EGTA, 0 Mg²⁺

$V_m = -70$

$V_m = -160$

100 pA

4 s

$V_m = +90$

100 pA

2 s

Figure 3. Voltage gating is intrinsic to Cx46 hemichannels. Shown are multichannel cell-attached patch recordings from a Cx46-expressing oocyte with (A) 1 mM Mg²⁺ present in the patch pipette and (B) with no added Mg²⁺ in the patch pipette. In both cases, Ca²⁺ was buffered to very low levels with EGTA. When the extracellular solution (patch pipette solution) contained 1 mM Mg²⁺, membrane hyperpolarization to −70 mV and depolarization to +90 mV produced reductions in current characteristic of loop gating and V_j gating, respectively. Currents were leak subtracted (dotted lines designate the 0 current level). When the extracellular solution was essentially devoid of external divalent cations, V_j gating at +90 mV was unaffected and loop gating at −70 mV was abolished, but application of a very large hyperpolarizing step to −160 mV caused a robust and rapid decrease in current. Although the current clearly declined toward zero, it remained very flickery and noisy. All currents were filtered at 1 kHz and data were acquired at 5 kHz.

−70 mV, closure was robust. Positive membrane voltages also elicited gating of Cx46 hemichannels, but the characteristics differed substantially. Most notably, conductance did not decline to zero, leaving a substantial residual conductance. As previously described, closure at positive and negative voltages occur by different gating mechanisms. At positive voltages there is gating to a residual subconductance state by a mechanism we have termed V_j gating; at negative voltages Cx46 hemichannels gate fully closed by a mechanism we have termed loop gating (Trexler et al., 1996; Bukauskas and Verselis, 2004). In Cx46, these gating mechanisms are distinguished not only by voltage polarity and the degree of hemichannel closure, but also by characteristically different gating transitions. V_j gating transitions are rapid and not resolved, typical of ion channel gating, whereas loop gating transitions consist of passage through a series of transient subconducting states en route to full closure/opening. Examples are shown in Fig. 2 C at −70 and +40 mV.

When external Mg²⁺ was omitted from the external solution, gating in response to voltage was substantially altered, but only at negative membrane voltages (Fig. 2 B). V_j gating at positive membrane voltages remained unchanged whereas the robust closure due to loop gating at negative membrane potentials did not occur. This effect on gating is also illustrated in a different patch recording containing multiple Cx46 hemichannels in which application of a large positive voltage to +90 mV produced the characteristic decrease to a residual level and was essentially the same when external Mg²⁺ was present or absent (Fig. 3). Application of a large negative membrane voltage of −70 mV produced robust clo-

sure in the presence of 1 mM external Mg²⁺, but little or no closure in the absence of added Mg²⁺. However, when a very large hyperpolarizing voltage to −160 mV was applied, current decreased robustly. Notably, however, the current at steady state, although substantially reduced, remained very noisy in contrast to the relatively quiet baseline typically observed with closure in the presence of divalent cations, in this case Mg²⁺. These results demonstrate that V_j gating is not affected when the external divalent cation concentration is reduced and further suggests that loop gating, although modulated by external divalent cations, remains robust in their absence or at very low (submicromolar) concentrations.

Mg²⁺ Stabilizes Full Closures Associated with Loop Gating

To better examine the action of divalent cations at negative membrane potentials, we recorded from patches containing only a single Cx46 hemichannel. Fig. 4 shows 30-s traces from an excised, outside-out patch recorded at various negative membrane potentials with and without Mg²⁺ added to the bath; free Ca²⁺ was buffered to submicromolar levels with EGTA. When no Mg²⁺ was present on the extracellular side, the hemichannel still clearly exhibited voltage dependence with hyperpolarization. Although very large negative membrane potentials were required to reduce open probability (P_o), it nonetheless decreased in a voltage-dependent manner evident as increasingly less time spent in the fully open state (see all points histograms to the right of each trace). Interestingly, the hemichannel did not spend much time in a clearly defined closed state either, displaying nearly continuous noisy fluctuations in current from the baseline that varied in amplitude, consistent with the noisy baseline observed in patches containing
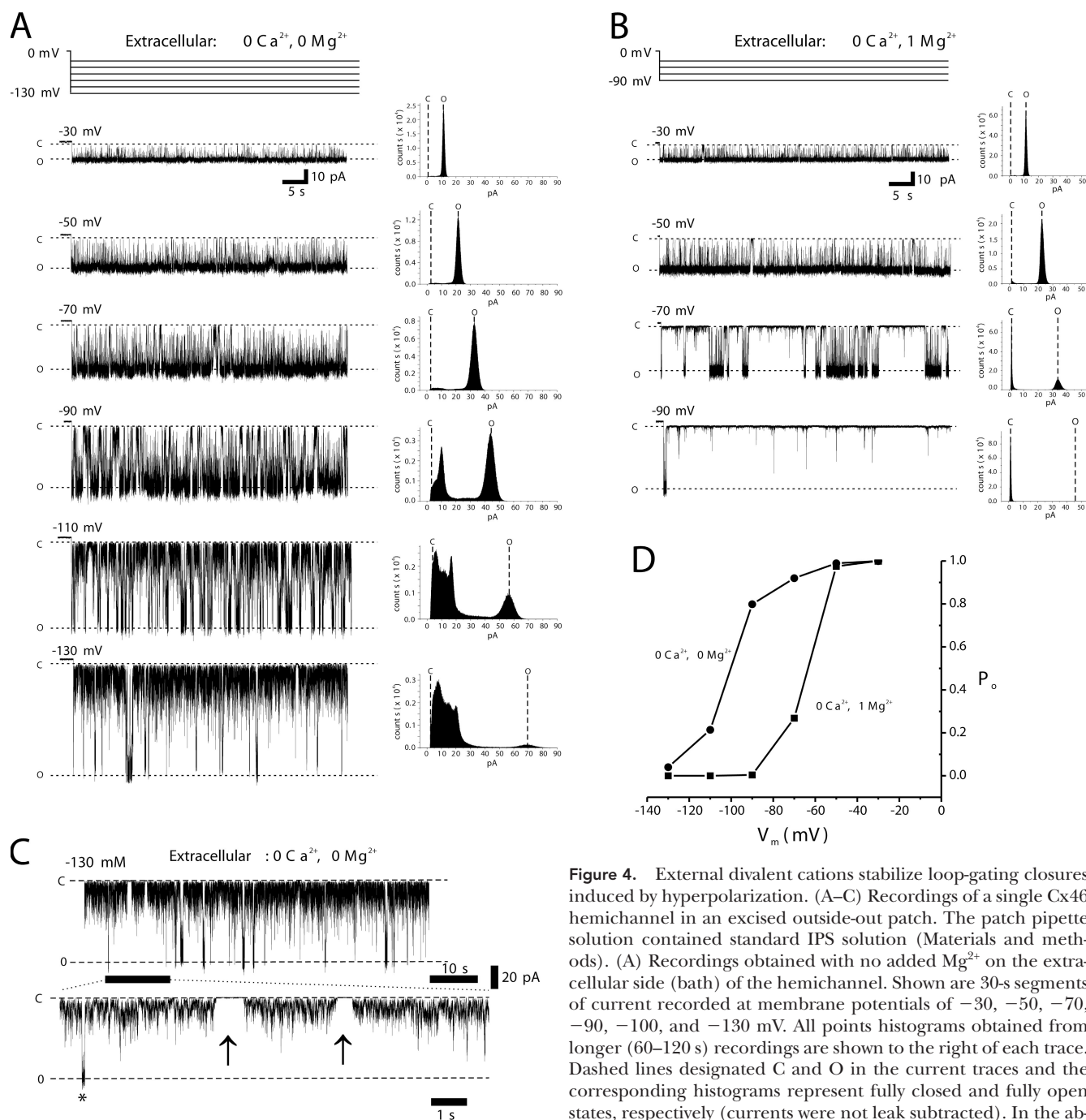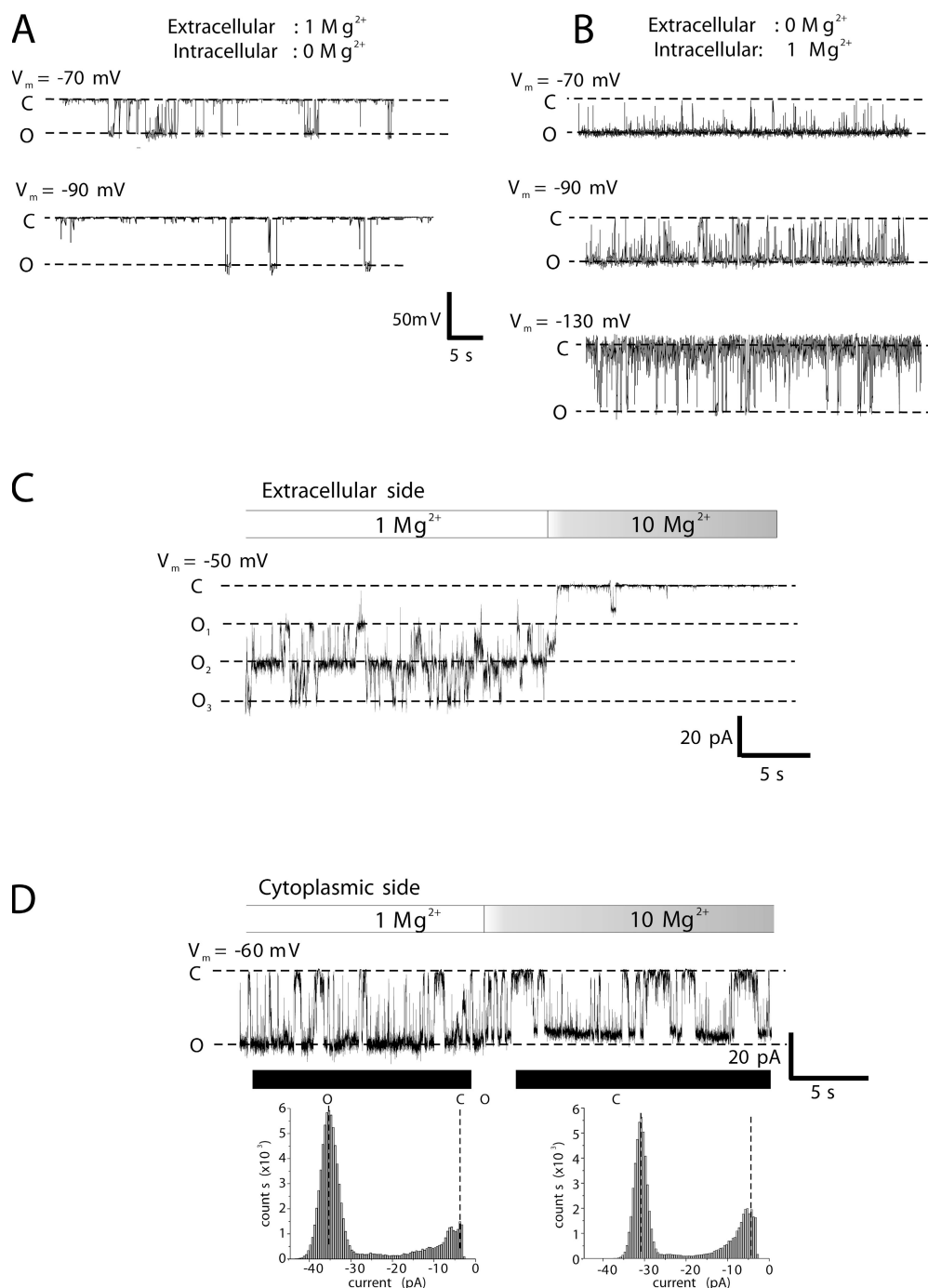
Figure 4. External divalent cations stabilize loop-gating closures induced by hyperpolarization. (A–C) Recordings of a single Cx46 hemichannel in an excised outside-out patch. The patch pipette solution contained standard IPS solution (Materials and methods). (A) Recordings obtained with no added Mg^{2+} on the extracellular side (bath) of the hemichannel. Shown are 30-s segments of current recorded at membrane potentials of -30, -50, -70, -90, -100, and -130 mV. All points histograms obtained from longer (60–120 s) recordings are shown to the right of each trace. Dashed lines designated C and O in the current traces and the corresponding histograms represent fully closed and fully open states, respectively (currents were not leak subtracted). In the absence of divalent cations, the hemichannel clearly exhibits voltage dependence with hyperpolarization tending toward closure. At large hyperpolarizing voltages, the hemichannel rarely resides in the fully open state and exhibits very noisy flickering (see spread in the histograms away from the fully closed state). (B) Addition of 1 mM Mg^{2+} to the bath dramatically changed the behavior of the hemichannel. Stable, long-duration closures became evident and considerably more modest voltages produced closure (compare histograms at -90 mV with and without added Mg^{2+}). (C) View of the current trace recorded at -130 mV with no added Mg^{2+} at an expanded time scale. The solid bar indicates the segment of the trace that was expanded below. The noisy flickering associated with closure can be seen to be occasionally interrupted by full closures that are quiet (indicated by arrows). Asterisk denotes a brief opening event. (D) Plots of P_o vs. V_m obtained from the recordings in A and B. P_o represents the fraction of time spent in the fully open state (see Materials and methods). These data illustrate that in solutions essentially devoid of divalent cations, voltage dependence remains robust although significantly shifted in the hyperpolarizing direction. Currents were filtered at 2 kHz and data were acquired at 10 kHz.

multiple active hemichannels (Fig. 3 B). When viewed at an expanded time scale, the noisy fluctuating current was occasionally interrupted by full closures to a quiet base-line (Fig. 4 C, quiet baseline indicated by arrows and full openings by asterisks). Changing the Ca^{2+}/EGTA ratio so that the calculated free Ca^{2+} varied between $\sim$2 and

Figure 5. The binding site for divalent cations is extracellular. (A) Recording of a single hemichannel in an outside-out patch configuration with 1 mM Mg^{2+} on the extracellular side and no added Mg^{2+} on the cytoplasmic side. Openings observed at -70 mV became more sporadic and brief upon hyperpolarization to -90 mV. (B) Recording of a single hemichannel in an outside-out patch configuration with no added Mg^{2+} on the extracellular side and 1 mM Mg^{2+} on the cytoplasmic side. In the presence of 1 mM Mg^{2+} on the cytoplasmic side, the hemichannel largely remained open at -70 mV. Closure increased with hyperpolarization to -90 mV and was robust at -130 mV. These large hyperpolarizing voltages would tend to prevent Mg^{2+}, which is present only on the cytoplasmic side, from entering the pore inconsistent with voltage-dependent entry of Mg^{2+} leading to block. (C) Patch recording containing three active Cx46 hemichannels in an outside-out patch configuration. Membrane potential was held constant at -50 mV. Starting in symmetric conditions, with 1 mM Mg^{2+} present on both sides, perfusion of a solution containing 10 mM Mg^{2+} into the bath (as indicated), which exposed the extracellular side to a high concentration of Mg^{2+}, produced rapid and robust closure. (D) The same experimental paradigm as in C applied to an inside-out patch containing a single hemichannel. Perfusing a solution containing 10 mM Mg^{2+} into the bath, which now exposed the cytoplasmic side to a high concentration of Mg^{2+}, did not appreciably affect hemichannel behavior except for a small reduction in the magnitude of the unitary current. Shown below the recording are histograms taken from the indicated segments (solid bars) before and after application of 10 mM Mg^{2+}. All currents were leak subtracted. Dashed lines indicate fully open (O) and fully closed (C) states. Currents were filtered at 1 kHz and data were acquired at 5 kHz.

10 nM did not appear to change the number of full closures to a quiet baseline (unpublished data).

In the presence of 1 mM Mg^{2+}, the behavior of the hemichannel differed significantly (Fig. 4 B). First, the hemichannel closed at more modest hyperpolarizations (compare histograms at -90 mV with and without Mg^{2+}), consistent with the shift observed in macroscopic recordings, and second, the noisy baseline current was transformed into a more stable, quiet baseline current. Although there were still noisy fluctuations from the baseline, they were intermittent and reduced in extent. Plots of P_o vs. V_m calculated from 60–120-s recordings of the same patch illustrate the large shift in activation by external Mg^{2+} (Fig. 4 D). Mean values for V_0, the voltage

at which P_0 is 0.5, in the presence or absence of extracellular Mg^{2+} were -59 ± 7 mV ($n = 5$ patches) and -105 ± 11 ($n = 6$ patches). Although shifted, voltage dependence with no added external Mg^{2+} remained comparably steep.

Mg^{2+} Is only Effective from the Extracellular Side

The results, thus far, suggest that divalent cations selectively modify loop gating rather than acting as open channel blockers or gating particles. To further test the viability of open channel block, we examined the sidedness of the divalent cation effect, specifically whether Mg^{2+} was effective at closing the hemichannel from either side of the membrane as would be expected for a blocking site in the aqueous pore. Fig. 5 (A and B) shows recordings of single Cx46 hemichannels in excised patches. Bath and pipette solutions contained EGTA to chelate Ca^{2+}. Mg^{2+} (1 mM) was present in the bath solution, but not the pipette solution, resulting in exposure of only one side of the hemichannel to divalent cations upon excision of the patch. In an outside-out patch, where the extracellular face of the hemichannel was exposed to the bath and hence 1 mM Mg^{2+}, open probability was low at a membrane potential of -70 mV (Fig. 5 A). Upon hyperpolarizing further to -90 mV, openings became very brief and infrequent. In dramatic contrast, in an inside-out patch, when the cytoplasmic face of the hemichannel was exposed to the bath and hence 1 mM Mg^{2+}, the hemichannel remained largely open at -70 mV (Fig. 5 B). Further hyperpolarization to -90 mV and then -130 mV progressively reduced open probability. Hyperpolarization of the membrane, in this case, required depolarization of the patch pipette, which would tend to keep divalent cations that are on the bath (cytoplasmic) side from entering the pore. Thus, the voltage-dependent reduction in open probability observed with membrane hyperpolarization and Mg^{2+} present only on the cytoplasmic side is the wrong polarity to be caused by voltage-dependent entry of Mg^{2+} into the pore leading to block.

We also examined the effect of increasing the concentration of Mg^{2+} beyond 1 mM. Exposure of the extracellular side of Cx46 hemichannels to 10 mM Mg^{2+} rapidly and effectively closed them (Fig. 5 C). In contrast, exposure of the cytoplasmic side to 10 mM Mg^{2+} did not have an appreciable effect except for a small reduction in the magnitude the unitary current (Fig. 5 D). In the example shown, amplitude histograms taken from the indicated segments illustrate the reduction in current magnitude and little change in the distribution of states. The effect of 10 mM Mg^{2+} over a large voltage range is illustrated in single hemichannel I-V relations obtained by applying voltage ramps from -70 to $+70$ mV to excised patches (Fig. 6 A). The left traces were obtained from an inside-out patch containing a single hemichannel in which the Mg^{2+} concentration was 1 mM on both

sides. The middle and right traces were obtained from excised patches with Mg^{2+} elevated to 10 mM on the cytoplasmic and extracellular sides, respectively. Ensemble currents obtained from multiple ramps and patches are shown in Fig. 6 B. The presence of 10 mM Mg^{2+} on the cytoplasmic side had little effect on the single channel I-V relation. Both loop gating at negative membrane voltages and positive membrane voltage remained essentially similar. In contrast, the same concentration of Mg^{2+} applied to the extracellular side had a dramatic effect, keeping hemichannels closed at inside negative voltages; opening usually required depolarization to inside positive voltages, consistent with a large positive shift in activation. The apparent effect on V_j gating at positive voltages can be explained by interactions between the two gates, which lie in series along the channel pore. When external divalent cation concentrations are high, the loop gates can close or remain closed at more positive voltages, thereby changing the voltage sensed by the V_j gates and altering their tendency to close (Srinivas et al., 2005). For completeness, we also examined patches in which no added Mg^{2+} was present on the outside so that the only source of Mg^{2+} was on the cytoplasmic side. Again, exposure of the cytoplasmic side to 10 mM Mg^{2+} had no effect on the single hemichannel I-V relation (unpublished data). The small reduction in unitary conductance and the small shift in reversal potential (~ -2.1 mV) observed with 10 mM Mg^{2+} on the cytoplasmic side are consistent with Mg^{2+} being permeable to Cx46 hemichannels.

DISCUSSION

Connexin hemichannels constitute a less well-studied class of membrane ion channel that is strongly regulated by membrane voltage and divalent cations. Typically, hemichannels tend to open with depolarization and/or reduction in the levels of external divalent cations. More recently, however, it has been suggested that voltage dependence is not an intrinsic property of hemichannels, but rather is solely attributable to block/unblock by divalent cations. In Cx46 and Cx37 hemichannels, voltage-dependent gating was reported to be absent in solutions containing no added divalent cations (Ebihara et al., 2003; Puljung et al., 2004). A model to account for the effects of divalent cations in Cx46 hemichannels contains two binding sites, one in the pore that when bound blocks or closes the hemichannel in a voltage-dependent manner (Ebihara et al., 2003). Binding to a second site, accessible only from the extracellular side, stabilizes the blocked or closed state. Thus, it was deemed that there is no intrinsic voltage gating mechanism. In Cx37 hemichannels, polyvalent cations, including extracellular Ca^{2+}, Mg^{2+}, and Gd^{3+}, were proposed to traverse the length of the electric field and bind at the cytoplasmic end of the hemichannel pore (Puljung et al., 2004).
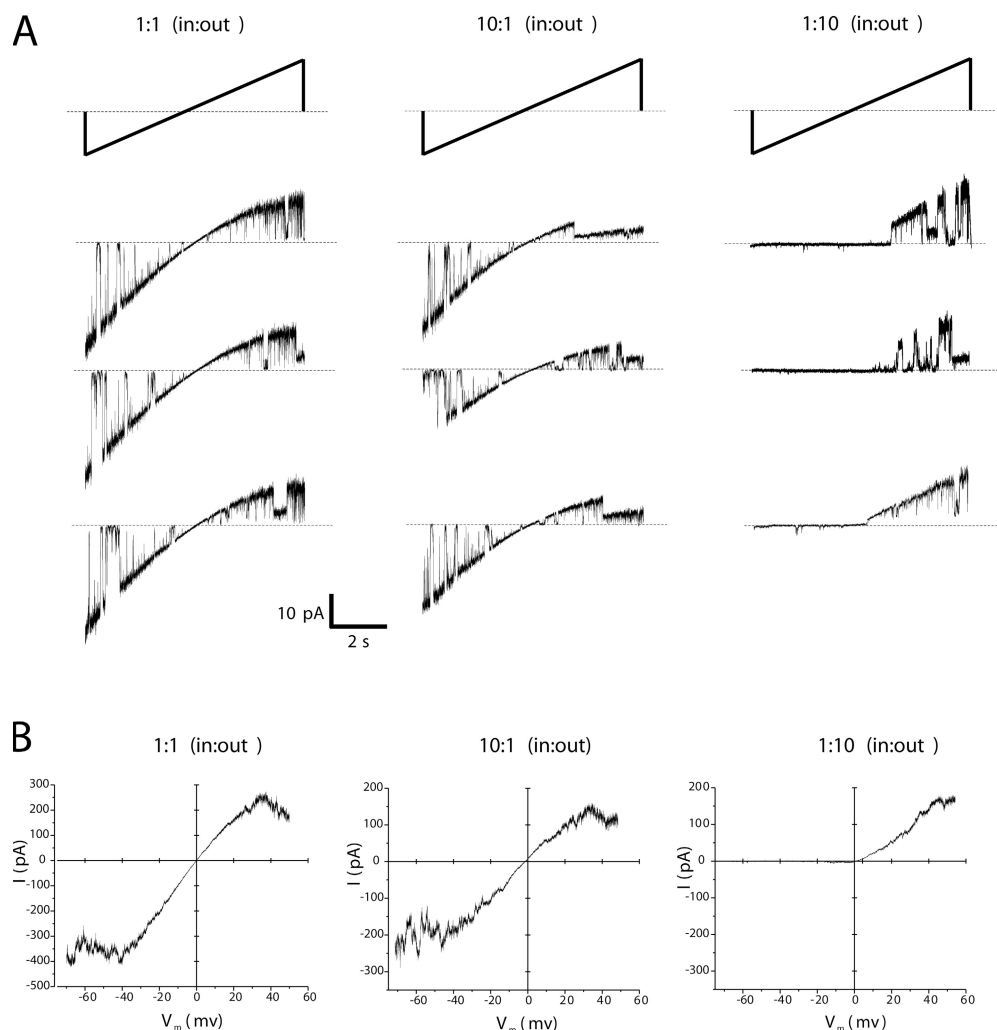
Figure 6. Examination of the effects of Mg^{2+} over a voltage range. (A) Single hemichannel currents obtained with 8-s voltage ramps from -70 to $+70$ mV applied to excised patches. Shown are examples of three current traces in response to voltage ramps applied in succession to a patch in which the Mg^{2+} concentration was 1 mM on both sides (left), elevated to 10 mM on the cytoplasmic (middle) and elevated to 10 mM on the extracellular (right). The currents were leak subtracted. (B) Current–voltage relationships of Cx46 hemichannels constructed from ensemble averaged currents from multiple patches in response to ±70 mV, 8-s voltage ramps applied to excised patches as shown in A. The I-V relationship with 10 mM Mg^{2+} on the cytoplasmic side was essentially similar to that obtained in symmetric 1 mM Mg^{2+}, except for a small reduction in unitary current and a small negative shift in E_{rev}. In contrast, the same concentration of Mg^{2+} applied to the extracellular side showed strong voltage dependence with hemichannels closing at inside negative voltages and opening at positive voltages. The strong voltage dependence of closure observed only when Mg^{2+} is elevated extracellularly but not cytoplasmically argues against a pore-blocking mechanism and is consistent with an extracellular modulatory site, which when bound with divalent cations causes a positive shift in activation to more positive voltages.

Macroscopic vs. Single Channel Recordings

Using single hemichannel recordings in excised patches where we could examine hemichannels in isolation and test the effectiveness of divalent cations from either side of the membrane, we find that a pore-blocking model is unlikely, at least for Cx46 hemichannels. In solutions containing no added Mg^{2+} and EGTA to reduce Ca^{2+} to submicromolar levels, we found that robust voltage dependence persisted and that the action of divalent cations was to selectively modulate one of two forms of intrinsic voltage-dependent gating that we have provisionally termed loop gating (Trexler et al., 1996; Verselis and Bukauskas, 2002; Bukauskas and Verselis, 2004). Although this selective action on loop gating was evident both in macroscopic and single hemichannel recordings, we wish to point out that when we examined the effects of Ca^{2+} and Mg^{2+} macroscopically, the results depended on the level of Cx46 expression. When currents were large (exceeding 5–10 μA), because of high levels of expressed connexin and/or exposure of oocytes to low levels of divalent cations, voltage dependence indeed weakened or even disappeared. In solutions containing no added Ca^{2+} or Mg^{2+}, when membrane conductances were usually elevated to very high levels (>10 μS), we typically did not observe voltage dependence at all over a large voltage range, negative and positive. Such effects in oocytes can be attributed to series access resistance whereby the effective voltage drop across the membrane is rendered nonuniform and reduced in magnitude due to significant contributions of cytoplasmic and extracellular resistances (Baumgartner et al., 1999). In addition, tight clustering of channels and possibly hemichannels can produce overlapping access pathways for each aqueous pore, creating the characteristics of a single, large diameter pore in which access resistance makes a larger relative contribution (Wilders and Jongsma, 1992; Hille et al., 1999). Weakening or loss of voltage dependence has been documented

in recordings of gap junctional currents from oocyte cell pairs exhibiting high junctional membrane conductances (Verselis et al., 1994). Thus, we conclude that we could not entirely rely on macroscopic recordings to assess the effects of low concentrations of divalent cations on connexin hemichannel gating. It is possible that series access resistance may be the basis for the apparent loss of hemichannel gating reported by Ebihara et al. (2003) and Puljung et al. (2004).

Divalent Cations, Pore Block, and Connexin Specificity

Both the persistence of gating in solutions containing no added Mg^{2+} and EGTA to chelate Ca^{2+} and the sidedness of the Mg^{2+} effect argue strongly against pore block as the mechanism by which divalent cations rapidly and reversible modulate Cx46 currents, at least in the concentration range we examined. Altering Mg^{2+} between 1 and 10 mM on the extracellular side had profound effects on open probability, whereas the same changes in Mg^{2+} on the cytoplasmic side had little effect, indicating that the binding site is certainly not on the cytoplasmic side of the hemichannel. In particular, when Mg^{2+} was elevated to 10 mM on the cytoplasmic side, the expectation for a pore-blocking mechanism would be that voltage dependence should reverse in sign as depolarization should now drive Mg^{2+} into the channel. We did not see evidence of such reversal of polarity, even when the extracellular side was exposed to a solution containing no added Mg^{2+} so that the only source of Mg^{2+} was through the pore from the cytoplasmic side. It is possible that access from the cytoplasmic side of the hemichannel is hindered in some way. However, this possibility would be difficult to reconcile for a channel with such a large pore that has been shown to be cation selective and permeable to large fluorescent dyes and large thiol reagents added to either side of the membrane (Pfahnl and Dahl, 1998; Trexler et al., 2000; Kronengold et al., 2003a,b) The V_j gate, which has been suggested to involve narrowing of the cytoplasmic vestibule (Ri et al., 1999), could conceivable block access when in the substate conformation, but there is little gating at positive voltages up to +35 mV and block is still absent from the cytoplasmic side. We also observed that addition of Mg^{2+} to the cytoplasmic side reduced unitary conductance and shifted the reversal potential in a direction consistent with Mg^{2+} permeability. Thus, it is unlikely that access to a blocking site in the pore is hindered from the cytoplasmic aspect of the hemichannel.

Our result differs from that of Pfahnl and Dahl (1999) who examined the effects of Ca^{2+} on Cx46 hemichannels in excised patches. Exposure of Cx46 hemichannels to high concentrations of Ca^{2+} (2.4 mM added) on either side of the membrane led to robust closure. In their hands, the voltage polarity that produced closure reversed when the side of Ca^{2+} application was reversed. These results led to the conclusion that Ca^{2+} enters and binds to a site inside the pore. An extension of having a binding site in the connexin pore is that cytoplasmic Ca^{2+} and Mg^{2+} would likely be effective at closing gap junction (cell–cell) channels as well. Although cytoplasmic Ca^{2+} has been shown regulate gap junction channels at concentrations as low as ∼150–300 nM, there is evidence that this modulation requires soluble intermediaries (Peracchia, 2004). For Cx43, intracellular Ca^{2+} elevated to the μM range did not cause uncoupling when calmodulin was inhibited (Lurtz and Louis, 2007), suggesting that Ca^{2+} itself is not a potent blocker. Also, Ca^{2+} permeability through gap junctions may contribute to the propagation of Ca^{2+} waves (Saez et al., 1989; Paemeleire et al., 2000). Elevating Ca^{2+} to the mM range on the cytoplasmic side has not been tested in gap junctions, but such high concentrations would be difficult to interpret because of secondary effects and deleterious effects on cell viability. Elevating Mg^{2+}, which is normally 1–3 mM inside cells, to as high as 10 mM did not produce block in Cx37 gap junction channels, but did alter gating kinetics more than predicted based on screening suggestive of binding (Ramanan et al., 1999). Permeability of hemichannels to Ca^{2+} has not been rigorously tested. In any case, the high concentration of cytoplasmic Ca^{2+} used in the studies of Pfahnl and Dahl (1999) may produce effects that are unrelated to loop gating. Thus, Ca^{2+} and Mg^{2+} could conceivably share a common extracellular site that functions to regulate loop gating and additional effects of high concentrations of Ca^{2+} may promote hemichannel closure by independent means. We were unable to obtain stable patches in solutions that did not contain EGTA or BAPTA and therefore could not reliably test the effects of μM concentrations of Ca^{2+} on single Cx46 hemichannels. Resolution awaits examination of the effects of Ca^{2+} at the single hemichannel level over a wide range of concentrations.

In Cx32 hemichannels, a ring of 12 Asp residues in the second extracellular loop, E2, consisting of D169 and D178 was reported to be the basis of Ca^{2+} regulation (Gomez-Hernandez et al., 2003). However, the reported affinity for external Ca^{2+} in this hemichannel is low compared with Cx46, with 50% reduction in current occurring at a concentration of 1.3 mM; affinity for Mg^{2+} is only modestly lower. Also, the proposed mechanism of action was reported to involve effects both on gating and conduction centered around a subconducting state. Pore block was proposed as one possible mechanism of action, but in Cx46, the first extracellular loop, E1, has been shown to contribute to the pore. Also, both D169 and D178 were necessary to maintain Ca^{2+} regulation in Cx32, but negative charges at both positions is not widely conserved among connexins. Thus, it may be that there are connexin-specific differences in divalent cation regulation and/or a multiplicity of actions over a wide concentration range.

Connexin Gating by Voltage

Our results indicate that loop and V_j gating are both intrinsic voltage-dependent mechanisms, with loop gating being that which is selectively modulated by extracellular divalent cations. The V_j gating mechanism has been proposed to involve movement of the N-terminal domain at the cytoplasmic end the channel, mediated by a proline-kink motif in the second transmembrane domain (Verselis et al., 1994; Ri et al., 1999). The result is a narrowing of the pore at the cytoplasmic end, i.e., the residual subconducting state. Consistent with this mechanism being intrinsically voltage dependent, charged amino acid substitutions in NT can reverse gating polarity, suggesting reversal of the sign of a voltage sensor (Verselis et al., 1994; Purnick et al., 2000). The molecular determinants of loop gating remain unknown, but there is the suggestion that this mechanism operates at the opposite end of the hemichannel, i.e., at the extracellular end. First, loop gating is robustly modulated by external, not internal, divalent cations. Second, studies using the substituted cysteine accessibility method in Cx46 hemichannels reported accessibility of residue L35 in the first transmembrane domain, TM1 (Zhou et al., 1997; Kronengold et al., 2003b). Closure of the loop gate appeared to block accessibility from the cytoplasmic side, suggesting the gate or the constriction that occurs with gating is located extracellular to this position (Pfahnl and Dahl, 1998). Finally, conformational changes at the surfaces of hemichannels examined using atomic force microscopy indicate that the extracellular pore entrance is significantly decreased in diameter upon addition of Ca^{2+} (Muller et al., 2002; Thimm et al., 2005). Whether this structural change is related to loop gating is unknown.

Divalent Cations as Modulators of Intrinsic Voltage-dependent Gating

Recordings at the single hemichannel level in solutions containing no added Mg^{2+} and EGTA revealed interesting features of loop gating. Although progressive hyperpolarization induced progressively less time spent in the fully open state, as expected for a voltage-dependent mechanism, Cx46 hemichannels did not spend much time fully closed either, but rather flickered nearly continuously between what may be poorly resolved subconductance states and/or a closed state. At the largest membrane voltage (-130 mV) that we could maintain a stable patch recording for an extended period of time, it was difficult to decipher clear conductance states, except for occasional and brief full openings (Fig. 4 C, asterisks) and occasional full closures to the baseline during which flickering was interrupted (Fig. 4 C, arrows). Typically, the full closures were brief, lasting tens of milliseconds or a few hundred milliseconds at best. Addition of extracellular divalent cations, in this case 1 mM Mg^{2+}, promoted full closures that lasted much

longer, many seconds. Flickering still occurred within these long closures but appeared as intermittent bursts in contrast to the nearly continuous flickering in the absence of added Mg^{2+}. We suggest that the full closures under very low divalent cation conditions represent spontaneous entry into a fully closed state rather than occasional binding resulting from trace amounts of divalent cations, because varying the Ca^{2+}/EGTA ratio such that the calculated free Ca^{2+} varied from ~ 2 to ~ 10 nM did not increase the frequency of the full closures (unpublished data).

We suggest the following regulatory mechanism in Cx46 hemichannels that combines effects of voltage and divalent cations. Hemichannels undergo a complex series of conformational changes from the fully open state to the fully closed state that constitutes loop gating. Some of the intermediate conformational states in loop gating are resolvable as short-lived subconductance states. This process is intrinsically voltage dependent, with hyperpolarization tending toward closure. Flickering from the fully closed state plausibly represents attempts at opening or partial opening. Thus, voltage drives the hemichannel to close, perhaps by initiating movements in the extracellular loops, but residence in a stable, fully closed state requires the binding of divalent cations to an extracellular site. In the absence of extracellular divalent cations, the hemichannel exhibits continuous transiting between the short-lived states that characterize loop gating transitions.

Possibilities for hemichannel function, both physiological and pathological, are growing in a number of tissues (Evans et al., 2006). Voltage and divalent cations are both involved in regulating hemichannels and it appears that changes in extracellular Ca^{2+} and membrane potential will likely combine to rapidly and reversibly regulate hemichannel opening in robust fashion. This study shows that an intimate association between divalent cations and voltage gating occurs through loop gating, a gating mechanism that is intrinsically voltage dependent as well as Ca^{2+}/Mg^{2+} dependent. In this view, loop gating is the mechanism responsible for opening hemichannels in the plasma membrane by depolarization, lowered extracellular Ca^{2+}, and, perhaps, by other conditions known to modulate hemichannel activity such as metabolic inhibition, intracellular pH and pharmacological agents (John et al., 1999; Trexler et al., 1999; Contreras et al., 2002; Trelles, M.P., and M. Srinivas. 2007. *Biophysical Society Meeting Abstracts, Biophysical Journal.* Supplement: 442a, Abstr. 2117). In addition, other factors, such as elevated extracellular K^+, have been shown to modulate Ca^{2+} sensitivity, thereby changing the dynamic range over which hemichannels can respond to divalent cations (Srinivas et al., 2006). The importance of having divalent cations as modulators rather than as gating particles is that the fundamental mechanism of closure is an intrinsic gating mechanism.

Thus, differences in loop gating among connexins may underlie apparent differences in Ca^{2+}/Mg^{2+} regulation. Also, without loop gating, divalent cations may not effectively regulate hemichannels, leading to cell death through influx of Ca^{2+} and/or efflux of ATP and other vital intracellular contents.

REFERENCES

Baumgartner, W., L. Islas, and F.J. Sigworth. 1999. Two-microelectrode voltage clamp of *Xenopus* oocytes: voltage errors and compensation for local current flow. *Biophys. J.* 77:1980–1991.

Bukauskas, F.F., and V.K. Verselis. 2004. Gap junction channel gating. *Biochim. Biophys. Acta.* 1662:42–60.

Contreras, J.E., H.A. Sanchez, E.A. Eugenin, D. Speidel, M. Theis, K. Willecke, F.F. Bukauskas, M.V. Bennett, and J.C. Saez. 2002. Metabolic inhibition induces opening of unapposed connexin 43 gap junction hemichannels and reduces gap junctional communication in cortical astrocytes in culture. *Proc. Natl. Acad. Sci. USA.* 99:495–500.

Draber, S., and R. Schultze. 1994. Detection of jumps in single-channel data containing subconductance levels. *Biophys. J.* 67:1404–1413.

Ebihara, L., and E. Steiner. 1993. Properties of a nonjunctional current expressed from a rat connexin46 cDNA in *Xenopus* oocytes. *J. Gen. Physiol.* 102:59–74.

Ebihara, L., X. Liu, and J.D. Pal. 2003. Effect of external magnesium and calcium on human connexin46 hemichannels. *Biophys. J.* 84:277–286.

Evans, W.H., E. De Vuyst, and L. Leybaert. 2006. The gap junction cellular internet: connexin hemichannels enter the signalling limelight. *Biochem. J.* 397:1–14.

Genetos, D.C., C.J. Kephart, Y. Zhang, C.E. Yellowley, and H.J. Donahue. 2007. Oscillating fluid flow activation of gap junction hemichannels induces ATP release from MLO-Y4 osteocytes. *J. Cell. Physiol.* 212:207–214.

Gomez-Hernandez, J.M., M. deMiguel, B. Larrosa, D. Gonzalez, and L.C. Barrio. 2003. Molecular basis of calcium regulation in connexin-32 hemichannels. *Proc. Natl. Acad. Sci. USA.* 100:16030–16035.

Hille, B., C.M. Armstrong, and R. MacKinnon. 1999. Ion channels: from idea to reality. *Nat. Med.* 5:1105–1109.

Huang, Y.J., Y. Maruyama, G. Dvoryanchikov, E. Pereira, N. Chaudhari, and S.D. Roper. 2007. The role of pannexin 1 hemichannels in ATP release and cell-cell communication in mouse taste buds. *Proc. Natl. Acad. Sci. USA.* 104:6436–6441.

John, S.A., R. Kondo, S.Y. Wang, J.I. Goldhaber, and J.N. Weiss. 1999. Connexin-43 hemichannels opened by metabolic inhibition. *J. Biol. Chem.* 274:236–240.

Kamermans, M., and I. Fahrenfort. 2004. Ephaptic interactions within a chemical synapse: hemichannel-mediated ephaptic inhibition in the retina. *Curr. Opin. Neurobiol.* 14:531–541.

Kamermans, M., I. Fahrenfort, K. Schultz, U. Janssen-Bienhold, T. Sjoerdsma, and R. Weiler. 2001. Hemichannel-mediated inhibition in the outer retina. *Science.* 292:1178–1180.

Kronengold, J., E.B. Trexler, F.F. Bukauskas, T.A. Bargiello, and V.K. Verselis. 2003a. Pore-lining residues identified by single channel SCAM studies in Cx46 hemichannels. *Cell Commun. Adhes.* 10:193–199.

Kronengold, J., E.B. Trexler, F.F. Bukauskas, T.A. Bargiello, and V.K. Verselis. 2003b. Single-channel SCAM identifies pore-lining residues in the first extracellular loop and first transmembrane domains of Cx46 hemichannels. *J. Gen. Physiol.* 122:389–405.

Locovei, S., J. Wang, and G. Dahl. 2006. Activation of pannexin 1 channels by ATP through P2Y receptors and by cytoplasmic calcium. *FEBS Lett.* 580:239–244.

Lurtz, M.M., and C.F. Louis. 2007. Intracellular calcium regulation of connexin43. *Am. J. Physiol. Cell Physiol.* 293:C1806–C1813.

Muller, D.J., G.M. Hand, A. Engel, and G.E. Sosinsky. 2002. Conformational changes in surface structures of isolated connexin 26 gap junctions. *EMBO J.* 21:3598–3607.

Paemeleire, K., P.E. Martin, S.L. Coleman, K.E. Fogarty, W.A. Carrington, L. Leybaert, R.A. Tuft, W.H. Evans, and M.J. Sanderson. 2000. Intercellular calcium waves in HeLa cells expressing GFP-labeled connexin 43, 32, or 26. *Mol. Biol. Cell.* 11:1815–1827.

Pelegrin, P., and A. Surprenant. 2006. Pannexin-1 mediates large pore formation and interleukin-1β release by the ATP-gated P2X7 receptor. *EMBO J.* 25:5071–5082.

Peracchia, C. 2004. Chemical gating of gap junction channels; roles of calcium, pH and calmodulin. *Biochim. Biophys. Acta.* 1662:61–80.

Pfahnl, A., and G. Dahl. 1998. Localization of a voltage gate in connexin46 gap junction hemichannels. *Biophys. J.* 75:2323–2331.

Pfahnl, A., and G. Dahl. 1999. Gating of cx46 gap junction hemichannels by calcium and voltage. *Pflugers. Arch.* 437:345–353.

Puljung, M.C., V.M. Berthoud, E.C. Beyer, and D.A. Hanck. 2004. Polyvalent cations constitute the voltage gating particle in human connexin37 hemichannels. *J. Gen. Physiol.* 124:587–603.

Purnick, P.E., S. Oh, C.K. Abrams, V.K. Verselis, and T.A. Bargiello. 2000. Reversal of the gating polarity of gap junctions by negative charge substitutions in the N-terminus of connexin 32. *Biophys. J.* 79:2403–2415.

Ramanan, S.V., P.R. Brink, K. Varadaraj, E. Peterson, K. Schirrmacher, and K. Banach. 1999. A three-state model for connexin37 gating kinetics. *Biophys. J.* 76:2520–2529.

Ri, Y., J.A. Ballesteros, C.K. Abrams, S. Oh, V.K. Verselis, H. Weinstein, and T.A. Bargiello. 1999. The role of a conserved proline residue in mediating conformational changes associated with voltage gating of Cx32 gap junctions. *Biophys. J.* 76:2887–2898.

Saez, J.C., J.A. Connor, D.C. Spray, and M.V. Bennett. 1989. Hepatocyte gap junctions are permeable to the second messenger, inositol 1,4,5-trisphosphate, and to calcium ions. *Proc. Natl. Acad. Sci. USA.* 86:2708–2712.

Schock, S.C., D. Leblanc, A.M. Hakim, and C.S. Thompson. 2008. ATP release by way of connexin 36 hemichannels mediates ischemic tolerance in vitro. *Biochem. Biophys. Res. Commun.* 368:138–144.

Srinivas, M., J. Kronengold, F.F. Bukauskas, T.A. Bargiello, and V.K. Verselis. 2005. Corrective studies of gating in Cx46 and Cx50 hemichannels and gap junction channels. *Biophys. J.* 88:1725–1739.

Srinivas, M., D.P. Calderon, J. Kronengold, and V.K. Verselis. 2006. Regulation of connexin hemichannels by monovalent cations. *J. Gen. Physiol.* 127:67–75.

Stout, C.E., J.L. Costantin, C.C. Naus, and A.C. Charles. 2002. Intercellular calcium signaling in astrocytes via ATP release through connexin hemichannels. *J. Biol. Chem.* 277:10482–10488.

Thimm, J., A. Mechler, H. Lin, S. Rhee, and R. Lal. 2005. Calcium-dependent open/closed conformations and interfacial energy maps of reconstituted hemichannels. *J. Biol. Chem.* 280:10646–10654.

Thompson, R.J., N. Zhou, and B.A. MacVicar. 2006. Ischemia opens neuronal gap junction hemichannels. *Science.* 312:924–927.

Trexler, E.B., M.V. Bennett, T.A. Bargiello, and V.K. Verselis. 1996. Voltage gating and permeation in a gap junction hemichannel. *Proc. Natl. Acad. Sci. USA.* 93:5836–5841.

Trexler, E.B., F.F. Bukauskas, M.V. Bennett, T.A. Bargiello, and V.K. Verselis. 1999. Rapid and direct effects of pH on connexins

revealed by the connexin46 hemichannel preparation. *J. Gen. Physiol.* 113:721–742.

Trexler, E.B., F.F. Bukauskas, J. Kronengold, T.A. Bargiello, and V.K. Verselis. 2000. The first extracellular loop domain is a major determinant of charge selectivity in connexin46 channels. *Biophys. J.* 79:3036–3051.

Verselis, V.K., and F.F. Bukauskas. 2002. Connexin-GFPs shed light on regulation of cell-cell communication by gap junctions. *Curr. Drug Targets.* 3:483–499.

Verselis, V.K., C.S. Ginter, and T.A. Bargiello. 1994. Opposite voltage gating polarities of two closely related connexins. *Nature.* 368:348–351.

Weissman, T.A., P.A. Riquelme, L. Ivic, A.C. Flint, and A.R. Kriegstein. 2004. Calcium waves propagate through radial glial cells and modulate proliferation in the developing neocortex. *Neuron.* 43:647–661.

Wilders, R., and H.J. Jongsma. 1992. Limitations of the dual voltage clamp method in assaying conductance and kinetics of gap junction channels. *Biophys. J.* 63:942–953.

Ye, Z.C., M.S. Wyeth, S. Baltan-Tekkok, and B.R. Ransom. 2003. Functional hemichannels in astrocytes: a novel mechanism of glutamate release. *J. Neurosci.* 23:3588–3596.

Zhao, H.B., N. Yu, and C.R. Fleming. 2005. Gap junctional hemichannel-mediated ATP release and hearing controls in the inner ear. *Proc. Natl. Acad. Sci. USA.* 102:18724–18729.

Zhou, X.W., A. Pfahnl, R. Werner, A. Hudder, A. Llanes, A. Luebke, and G. Dahl. 1997. Identification of a pore lining segment in gap junction hemichannels. *Biophys. J.* 72:1946–1953.